Vol. 8 (2015) *Acta Physica Polonica B Proceedings Supplement* No 1

NEW RESULTS ON CHARMONIUM PHYSICS FROM BaBar*

Antimo Palano

on behalf of the BaBar Collaboration

INFN and University of Bari, Italy

(Received December 5, 2014)

We study the processes $\gamma\gamma \to K^+K^-\eta$ and $\gamma\gamma \to K^+K^-\pi^0$ using a data sample of 519 fb^{-1} recorded with the BaBar detector. We observe $\eta_c \to K^+K^-\pi^0$ and $\eta_c \to K^+K^-\eta$ decays, measure their relative branching fraction, and perform a Dalitz plot analysis for each decay. We study the rare B-meson decays $B^{\pm,0} \to J/\psi K^+K^-K^{\pm,0}$, $B^{\pm,0} \to J/\psi\phi K^{\pm,0}$, and search for $B^0 \to J/\psi\phi$ finding no evidence of a signal. We present new measurements of branching fractions and a study of the $J/\psi\phi$ mass distribution in search of new charmonium-like states.

DOI:10.5506/APhysPolBSupp.8.79

PACS numbers: 13.25.Hw, 13.25.Gv, 14.40.Nd, 14.40.Rt

1. Dalitz plot analysis of $\eta_c \to K^+K^-\eta$ and $\eta_c \to K^+K^-\pi^0$ in two-photon interactions

Scalar mesons are still a puzzle in light-meson spectroscopy: there are too many states and they are not consistent with the quark model. In particular, the $f_0(1500)$ and $f_0(1710)$ resonances, discovered in $\bar{p}p$ annihilations and J/ψ decays respectively, have been interpreted as scalar glueballs [1]. Another puzzling state is the $K_0^*(1430)$ resonance, never observed as a clear peak in the $K\pi$ mass spectrum [2]. In the present analysis, we study three-body η_c decays to pseudoscalar mesons produced in two-photon interactions and obtain results that are relevant to several issues in the light-meson spectroscopy.

Two-photon events, in which at least one of the interacting photons is not quasi-real, are strongly suppressed by the selection criteria described below. This implies that the allowed J^{PC} values of any produced resonances

* Talk presented at the EEF70 Workshop on Unquenched Hadron Spectroscopy: Non-Perturbative Models and Methods of QCD *vs.* Experiment, Coimbra, Portugal, September 1–5, 2014.

are $0^{\pm+}$, $2^{\pm+}$, 3^{++}, $4^{\pm+}$, ... [3]. Angular momentum conservation, parity conservation, and charge conjugation invariance imply that these quantum numbers also apply to the final state except that the $K^+K^-\eta$ and $K^+K^-\pi^0$ states cannot be in a $J^P = 0^+$ state.

1.1. Mass spectra

In this analysis [4], we select events in which the e^+ and e^- beam particles are scattered at small angles and are undetected in the final state. We study the following reactions

$$\gamma\gamma \rightarrow K^+K^-\eta\,, \qquad (\eta \rightarrow \gamma\gamma)\,, \tag{1}$$
$$\gamma\gamma \rightarrow K^+K^-\eta\,, \qquad \left(\eta \rightarrow \pi^+\pi^-\pi^0\right)\,, \tag{2}$$

and

$$\gamma\gamma \rightarrow K^+K^-\pi^0\,. \tag{3}$$

We define $p_{\rm T}$ as the magnitude of the vector sum of the transverse momenta, in the e^+e^- rest frame, of the final-state particles with respect to the beam axis. Since well-reconstructed two-photon events are expected to have low values of $p_{\rm T}$, we require $p_{\rm T} < 0.05$ GeV/c.

Figure 1 (a) shows the $K^+K^-\eta$ mass spectrum, summed over the two η-decay modes, before applying the efficiency correction. There are 2950 events in the mass region between 2.7 and 3.8 GeV/c^2 of which 73% are from the $\eta \rightarrow \gamma\gamma$ decay mode and 27% are from the $\eta \rightarrow \pi^+\pi^-\pi^0$ decay mode. We observe a strong η_c signal and a small enhancement at the position of the $\eta_c(2S)$. We perform a simultaneous fit to the $K^+K^-\eta$ mass spectra for the two η decay modes. For each resonance, the mass and width are constrained to take the same fitted values in both distributions. Backgrounds are described by second-order polynomials, and each resonance is represented by a simple Breit–Wigner function convolved with the corresponding resolution function. Figure 1 (a) shows the fit result, and Table I summarizes the η_c and $\eta_c(2S)$ parameter values.

The $K^+K^-\pi^0$ mass spectrum is shown in Fig. 1 (b). There are 23 720 events in the mass region between 2.7 and 3.9 GeV/c^2. We observe a strong η_c signal and a small signal at the position of the $\eta_c(2S)$ on top of a sizeable background. In addition, we allow for the presence of a residual J/ψ contribution modeled as a simple Gaussian function. Figure 1 (b) shows the fit to the $K^+K^-\pi^0$ mass spectrum, and Table I summarizes the resulting η_c and $\eta_c(2S)$ parameter values.

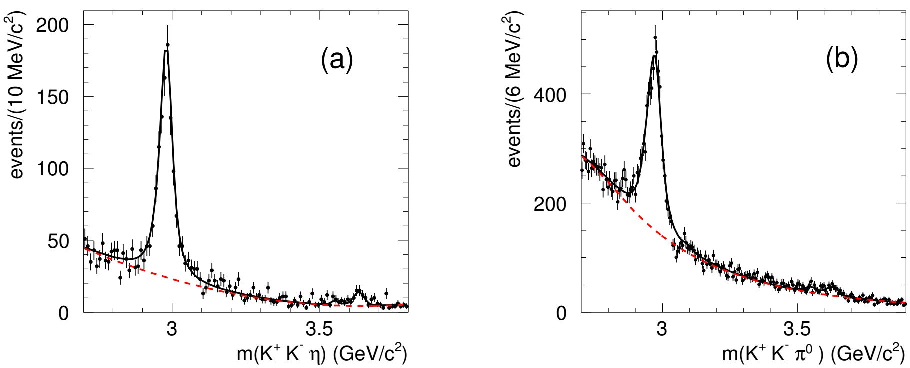

Fig. 1. (a) The $K^+K^-\eta$ mass spectrum summed over the two η-decay modes. (b) The $K^+K^-\pi^0$ mass spectrum. In each figure, the solid curve shows the total fitted function and the dashed curve shows the fitted background contribution.

TABLE I

Fitted η_c and $\eta_c(2S)$ parameter values. The first uncertainty is statistical and the second is systematic.

Resonance	Mass [MeV/c^2]	Γ [MeV]
$\eta_c \to K^+K^-\eta$	$2984.1 \pm 1.1 \pm 2.1$	$34.8 \pm 3.1 \pm 4.0$
$\eta_c \to K^+K^-\pi^0$	$2979.8 \pm 0.8 \pm 3.5$	$25.2 \pm 2.6 \pm 2.4$
$\eta_c(2S) \to K^+K^-\eta$	$3635.1 \pm 5.8 \pm 2.1$	11.3 (fixed)
$\eta_c(2S) \to K^+K^-\pi^0$	$3637.0 \pm 5.7 \pm 3.4$	11.3 (fixed)

We compute the ratios of the branching fractions for η_c and $\eta_c(2S)$ decays to the $K^+K^-\eta$ final state compared to the respective branching fractions to the $K^+K^-\pi^0$ final state. We calculate the weighted mean of the η_c branching-ratio estimates for the two η decay modes and obtain

$$\mathcal{R}(\eta_c) = \frac{\mathcal{B}\,(\eta_c \to K^+K^-\eta)}{\mathcal{B}\,(\eta_c \to K^+K^-\pi^0)} = 0.571 \pm 0.025 \pm 0.051\,, \qquad (4)$$

which is consistent with the BESIII measurement of 0.46 ± 0.23 [5]. Since the sample size for $\eta_c(2S) \to K^+K^-\eta$ decays with $\eta \to \pi^+\pi^-\pi^0$ is small, we use only the $\eta \to \gamma\gamma$ decay mode, and obtain

$$\mathcal{R}(\eta_c(2S)) = \frac{\mathcal{B}\,(\eta_c(2S) \to K^+K^-\eta)}{\mathcal{B}\,(\eta_c(2S) \to K^+K^-\pi^0)} = 0.82 \pm 0.21 \pm 0.27\,. \qquad (5)$$

1.2. Dalitz plot analysis of $\eta_c \to K^+K^-\eta$

We perform a Dalitz plot analysis of the $K^+K^-\eta$ and system in the η_c mass region using unbinned maximum likelihood fits. We define the η_c signal region as the range of 2.922–3.036 GeV/c^2. This region contains 1161 events with $(76.1 \pm 1.3)\%$ purity, defined as $S/(S+B)$, where S and B indicate the number of signal and background events. Figure 2 (left) shows the Dalitz plot for the η_c signal region and Fig. 3 shows the Dalitz plot projections.

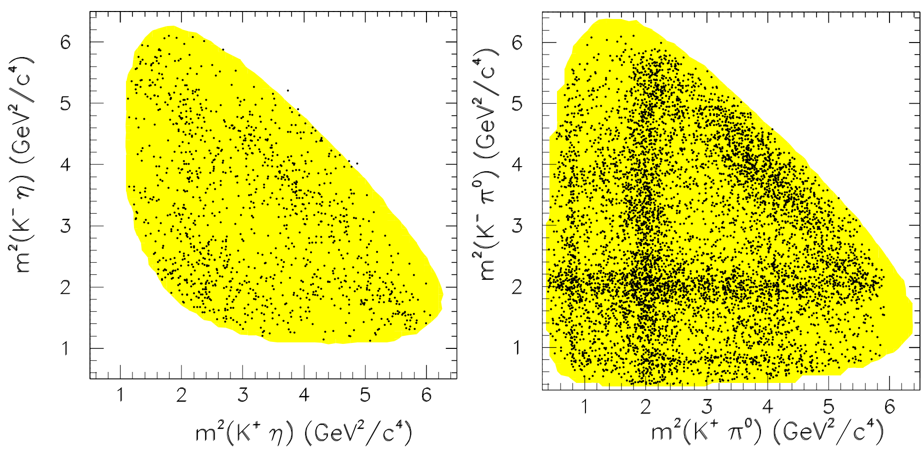

Fig. 2. (Left) Dalitz plot for the $\eta_c \to K^+K^-\eta$ events in the signal region. (Right) Dalitz plot for the events in the $\eta_c \to K^+K^-\pi^0$ signal region. The shaded area denotes the accessible kinematic region.

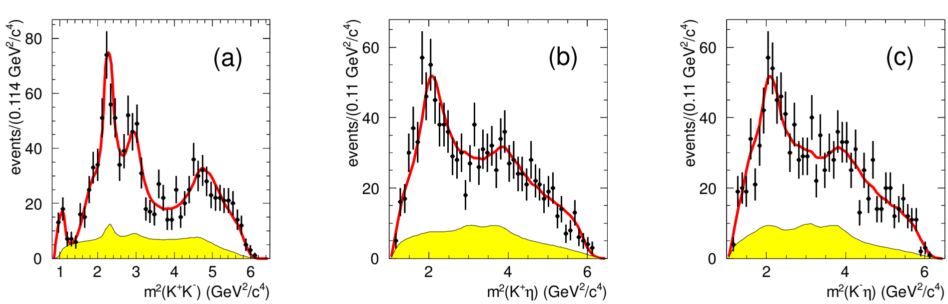

Fig. 3. The $\eta_c \to K^+K^-\eta$ Dalitz plot projections. The superimposed curves result from the Dalitz plot analysis described in the text. The shaded regions show the background estimates obtained by interpolating the results of the Dalitz plot analyses of the sideband regions.

We observe signals in the K^+K^- projections corresponding to the $f_0(980)$, $f_0(1500)$, $f_0(1710)$, and $f_0(2200)$ states. We also observe a broad signal in the 1.43 GeV/c^2 mass region in the $K^+\eta$ and $K^-\eta$ projections. Table II summarizes the fit results for the amplitude fractions and phases. We note that the $f_0(1500)\eta$ amplitude provides the largest contribution. We also observe important contributions from the $K_0^*(1430)^+K^-$, $f_0(980)\eta$, $f_0(2200)\eta$, and $f_0(1710)\eta$ channels. In addition, the fit requires a sizeable *NR* contribution. The sum of the fractions for this η_c decay mode is consistent with 100%.

TABLE II

Results of the Dalitz plot analysis of the $\eta_c \to K^+K^-\eta$ channel.

Final state	Fraction [%]	Phase [radians]
$f_0(1500)\eta$	23.7 ± 7.0 ± 1.8	0.
$f_0(1710)\eta$	8.9 ± 3.2 ± 0.4	2.2 ± 0.3 ± 0.1
$K_0^*(1430)^+K^-$	16.4 ± 4.2 ± 1.0	2.3 ± 0.2 ± 0.1
$f_0(2200)\eta$	11.2 ± 2.8 ± 0.5	2.1 ± 0.3 ± 0.1
$K_0^*(1950)^+K^-$	2.1 ± 1.3 ± 0.2	−0.2 ± 0.4 ± 0.1
$f_2'(1525)\eta$	7.3 ± 3.8 ± 0.4	1.0 ± 0.1 ± 0.1
$f_0(1350)\eta$	5.0 ± 3.7 ± 0.5	0.9 ± 0.2 ± 0.1
$f_0(980)\eta$	10.4 ± 3.0 ± 0.5	−0.3 ± 0.3 ± 0.1
NR	15.5 ± 6.9 ± 1.0	−1.2 ± 0.4 ± 0.1
Sum	100.0 ± 11.2 ± 2.5	
χ^2/ν	87/65	

1.3. Dalitz plot analysis of $\eta_c \to K^+K^-\pi^0$

We define the η_c signal region as the range of 2.910–3.030 GeV/c^2, which contains 6710 events with (55.2 ± 0.6)% purity. Figure 2 (right) shows the Dalitz plot for the η_c signal region, and Fig. 4 shows the corresponding Dalitz plot projections.

We observe an enhancement in the low mass region of the K^+K^- mass spectrum due to the presence of the $a_0(980)$, $a_2(1320)$, and $a_0(1450)$ resonances. The $K^\pm\pi^0$ mass spectrum is dominated by the $K_0^*(1430)$ resonance. We also observe $K^*(892)$ signals in the $K^\pm\pi^0$ mass spectrum in both the signal and sideband regions. Table III summarizes the amplitude fractions and phases obtained from the fit. The Dalitz plot analysis shows a dominance of scalar meson amplitudes with small contributions from spin-two resonances. The $K^*(892)$ contribution is consistent with originating entirely from the background. We note the presence of a sizeable non-resonant contribution. However, in this case, the sum of the fractions is significantly

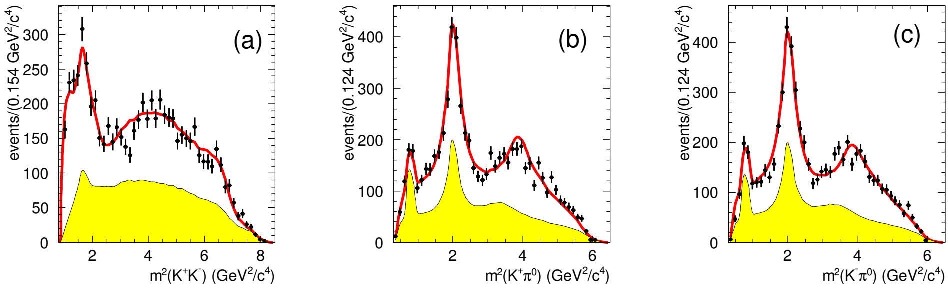

Fig. 4. The $\eta_c \to K^+K^-\pi^0$ Dalitz plot projections. The superimposed curves result from the Dalitz plot analysis described in the text. The shaded regions show the background estimates obtained by interpolating the results of the Dalitz plot analyses of the sideband regions.

lower than 100%, indicating important interference effects. Figure 4 shows the fit projections superimposed on the data, and good agreement is apparent for all projections. In the Dalitz plot analyses of $\eta_c \to K^+K^-\pi^0$, we perform a likelihood scan to obtain the best-fit parameters for the $K_0^*(1430)$. We obtain

$$\begin{aligned} m(K_0^*(1430)) &= 1438 \pm 8 \pm 4 \ \text{MeV}/c^2\,, \\ \Gamma(K_0^*(1430)) &= 210 \pm 20 \pm 12 \ \text{MeV}\,. \end{aligned} \tag{6}$$

TABLE III

Results of the Dalitz plot analysis of the $\eta_c \to K^+K^-\pi^0$ channel.

Final state	Fraction [%]	Phase [radians]
$K_0^*(1430)^+K^-$	$33.8 \pm 1.9 \pm 0.4$	0.
$K_0^*(1950)^+K^-$	$6.7 \pm 1.0 \pm 0.3$	$-0.67 \pm 0.07 \pm 0.03$
$a_0(980)\pi^0$	$1.9 \pm 0.1 \pm 0.2$	$0.38 \pm 0.24 \pm 0.02$
$a_0(1450)\pi^0$	$10.0 \pm 2.4 \pm 0.8$	$-2.4 \pm 0.05 \pm 0.03$
$a_2(1320)\pi^0$	$2.1 \pm 0.1 \pm 0.2$	$0.77 \pm 0.20 \pm 0.04$
$K_2^*(1430)^+K^-$	$6.8 \pm 1.4 \pm 0.3$	$-1.67 \pm 0.07 \pm 0.03$
NR	$24.4 \pm 2.5 \pm 0.6$	$1.49 \pm 0.07 \pm 0.03$
Sum	$85.8 \pm 3.6 \pm 1.2$	
χ^2/ν	212/130	

The observation of the $K_0^*(1430)$ in the $K\eta$ and $K\pi^0$ decay modes permits a measurement of the corresponding branching ratio. We thus obtain

$$\frac{\mathcal{B}(K_0^*(1430) \to \eta K)}{\mathcal{B}(K_0^*(1430) \to \pi K)} = 0.092 \pm 0.025^{+0.010}_{-0.025}\,. \tag{7}$$

In Ref. [6], this small value is understood in the context of an SU(3) model with octet-singlet mixing of the η and η' [7]. In the present analysis, we obtain a θ_p mixing angle of $(3.1^{+3.3}_{-5.0})^\circ$, which differs by about 2.9 standard deviations from the result obtained from the $K_2^*(1430)$ branching ratio.

2. Study of $B^{\pm,0} \to J/\psi K^+K^-K^{\pm,0}$ and search for $B^0 \to J/\psi\phi$

Many charmonium-like resonances have been discovered in the past, revealing a spectrum too rich to interpret in terms of conventional mesons, expected from potential models [8].

In a search for exotic states, the CDF experiment studied the decay $B^+ \to J/\psi\phi K^+$, where $J/\psi \to \mu^+\mu^-$ and $\phi(1020) \to K^+K^-$, claiming the observation of a resonance labeled as the $X(4140)$ decaying to $J/\psi\phi$ [9]. They found evidence in the same decay mode for another resonance, labeled as the $X(4270)$ [10]. These results are confirmed by the CMS Collaboration [11].

We study the rare B-meson decays $B^{\pm,0} \to J/\psi K^+K^-K^{\pm,0}$, $B^{\pm,0} \to J/\psi\phi K^{\pm,0}$ using 469 million $B\overline{B}$ events collected at the $\Upsilon(4S)$ resonance. We select B-meson candidates using the energy difference ΔE in the center-of-mass frame and the beam-energy-substituted mass $m_{\rm ES}$ [12]. The selection requires $|\Delta E| < 30$ MeV and $|\Delta E| < 25$ MeV for B^+ and B^0 decays, respectively; the additional selection criterion $m_{\rm ES} > 5.2$ GeV/c^2 is required for the calculation of the BFs, while $m_{\rm ES} > 5.27$ GeV/c^2 is applied to select the signal region for the analysis of the invariant mass systems. An unbinned maximum likelihood fit to each $m_{\rm ES}$ distribution is performed to determine the yield and obtain a BF measurement. We use the sum of two functions to parametrize the $m_{\rm ES}$ distribution; a Gaussian function describes the signal, and an ARGUS function the background. Table IV summarizes the fitted yields obtained.

TABLE IV

Event yields, BF measurements ($\mathcal{B}$) and efficiencies (ϵ) for the different final states. For channels involving $K^0_{\rm S}$, the yields and efficiencies refer to $K^0_{\rm S} \to \pi^+\pi^-$, the BF includes the corrections for $K^0_{\rm S} \to \pi^0\pi^0$ and $K^0_{\rm L}$ decay. The $B^0 \to J/\psi\phi$ (B^0_ϕ) UL at 90% C.L. is listed at the end of the table.

B channel	Event yield	ϵ [%]	Corrected yield	$\mathcal{B}$ $(\times 10^{-5})$
B^+_{KKK}	290 ± 22	15.08 ± 0.04	1923 ± 146	$3.37 \pm 0.25 \pm 0.14$
$B^+_{\phi K}$	189 ± 14	13.54 ± 0.04	1396 ± 103	$5.00 \pm 0.37 \pm 0.15$
$B^0_{KKK^0}$	68 ± 13	10.35 ± 0.04	657 ± 126	$3.49 \pm 0.67 \pm 0.15$
$B^0_{\phi K^0}$	41 ± 7	10.10 ± 0.04	406 ± 69	$4.43 \pm 0.76 \pm 0.19$
B^0_{ϕ}	6 ± 4	31.12 ± 0.07	19 ± 13	< 0.101

2.1. Search for new resonances decaying to $J/\psi\phi$

To search for the two resonances claimed by the CDF Collaboration, we perform an unbinned maximum likelihood fit to the $B \to J/\psi\phi K$ decays. We model the resonances using S-wave relativistic Breit–Wigner (BW) functions with parameters fixed to the CDF values. The non-resonant contributions are represented by a constant term and no interference is allowed between the fit components. The decay of a pseudoscalar meson to two-vector states contains high spin contributions which could generate non-uniform angular distributions. However, due to the limited data sample, we do not include such angular terms, and assume that the resonances decay isotropically. The fit functions are weighted by the two-dimensional efficiency computed on the Dalitz plots.

Table V summarizes the results from the fits. We report the fit fractions for the two resonances, $f_{X(4140)}$ and $f_{X(4270)}$, the two-dimensional (2D) χ^2 computed on the Dalitz plot and the one-dimensional (1D) χ^2 computed on the $J/\psi\,\phi$ mass projection. We perform the fits using models with two resonances (labeled as model A), one resonance (models B and C), and no resonances (model D). The fit projections for fit A are displayed in Fig. 5, showing enhancements with a statistical significance smaller than 3.2σ for all fit models. All models provide a reasonably good description of the data, with χ^2 probability larger than 1%.

TABLE V

Fits to the $B \to J/\psi\,\phi K$ Dalitz plot. For each fit, the table gives the fit fraction for each resonance, and the 2D and 1D χ^2 values. The fractions are corrected for the background component.

Channel	Fit	$f_{X(4140)}$[%]	$f_{X(4270)}$[%]	2D χ^2/ν	1D χ^2/ν
B^+	A	9.2 ± 3.3	10.6 ± 4.8	12.7/12	6.5/20
	B	9.2 ± 2.9	0.	17.4/13	15.0/17
	C	0.	10.0 ± 4.8	20.7/13	19.3/19
	D	0.	0.	26.4/14	34.2/18
$B^0 + B^+$	A	7.3 ± 3.8	12.0 ± 4.9	8.5/12	15.9/19

Using the Feldman–Cousins method [13], we obtain the ULs at 90% C.L.

$$\mathcal{B}\big(B^+ \to X(4140)K^+\big) \times \mathcal{B}(X(4140) \to J/\psi\,\phi)/\mathcal{B}\big(B^+ \to J/\psi\,\phi K^+\big) < 0.133\,, \tag{8}$$

$$\mathcal{B}\big(B^+ \to X(4270)K^+\big) \times \mathcal{B}(X(4270) \to J/\psi\,\phi)/\mathcal{B}\big(B^+ \to J/\psi\,\phi K^+\big) < 0.181\,. \tag{9}$$

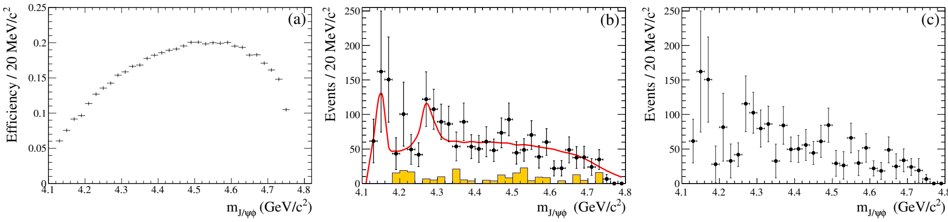

Fig. 5. (a) Average efficiency distribution as a function of the $J/\psi\phi$ mass for $B^+ \to J/\psi\phi K^+$. (b) Efficiency-corrected $J/\psi\phi$ mass spectrum for the combined B^+ and B^0 samples. The curve is the result from fit model A described in the text. (c) Efficiency-corrected and background-subtracted $J/\psi\phi$ mass spectrum for the combined B^+ and B^0 samples.

Figure 5 (a) shows the efficiency as a function of the $J/\psi\phi$ mass, obtained from a phase space simulation of the $B^+ \to J/\psi\phi K^+$ Dalitz plot. We observe a decrease of the efficiency in the $J/\psi\phi$ threshold region.

Figure 5 (b) shows the efficiency corrected $J/\psi\phi$ mass spectrum for the combined B^+ and B^0 samples. Finally, Fig. 5 (c) shows the efficiency corrected and background subtracted $J/\psi\phi$ mass spectrum for the combined B^+ and B^0 samples.

REFERENCES

[1] C. Amsler, F. Close, *Phys. Rev.* **D53**, 295 (1996).

[2] D. Aston *et al.* [LASS Collaboration], *Nucl. Phys.* **B296**, 493 (1988).

[3] C.N. Yang, *Phys. Rev.* **77**, 242 (1950).

[4] J.P. Lees *et al.* [BaBar Collaboration], *Phys. Rev.* **D89**, 112004 (2014).

[5] M. Ablikim *et al.* [BESIII Collaboration], *Phys. Rev.* **D86**, 092009 (2012).

[6] D. Aston *et al.* [LASS Collaboration], *Phys. Lett.* **B201**, 169 (1988).

[7] H.J. Lipkin, *Phys. Rev. Lett.* **46**, 1307 (1981).

[8] N. Brambilla *et al.* [Quarkonium Working Group], `arXiv:hep-ph/0412158`.

[9] T. Aaltonen *et al.* [CDF Collaboration], *Phys. Rev. Lett.* **102**, 242002 (2009).

[10] T. Aaltonen *et al.* [CDF Collaboration], `arXiv:1101.6058 [hep-ex]`.

[11] S. Chatrchyan *et al.* [CMS Collaboration], *Phys. Lett.* **B734**, 261 (2014).

[12] J.P. Lees *et al.* [BaBar Collaboration], *Phys. Rev.* **D85**, 052003 (2012).

[13] G.J. Feldman, R.D. Cousins, *Phys. Rev.* **D57**, 3873 (1998).